

## Novel Reduced Benzo[j]fluoranthren-3-ones from *Cladosporium* cf. *cladosporioides* with Cytokine Production and Tyrosine Kinase Inhibitory Properties

STEPHEN K. WRIGLEY\*, A. MARTYN AINSWORTH, DAVID A. KAU, STEVEN M. MARTIN, SANGEETA BAHL<sup>a</sup>, JENNY S. TANG<sup>a</sup>, DAVID J. HARDICK<sup>a,†</sup>, PHILIP RAWLINS<sup>a,††</sup>, ROYA SADHEGHI<sup>a,†††</sup> and MICHAEL MOORE<sup>a</sup>

Cubist Pharmaceuticals (UK) Limited,  
545 Ipswich Road, Slough, SL1 4EQ, UK  
<sup>a</sup> Xenova Limited,  
240 Bath Road, Slough, SL1 4EF, UK

(Received for publication February 13, 2001)

A series of reduced benzo[j]fluoranthren-3-ones (**1**~**4**) was isolated from fermentations of a fungal strain CBUK20700 (CBS 100220), classified as *Cladosporium* cf. *cladosporioides*, during a microbial extract screening programme to identify inhibitors of anti-CD28-induced interleukin-2 (IL-2) production by Jurkat E6-1 cells as potential immunosuppressive agents. These compounds were also found to be tyrosine kinase inhibitors. The structures of compounds **1**~**4** were elucidated by spectroscopic methods including the HMQC, HMBC and NOESY NMR experiments. The most potent compound in the series, (6*bS*,7*R*,8*S*)-7-methoxy-4,8,9-trihydroxy-1,6*b*,7,8-tetrahydro-2*H*-benzo[j]fluoranthren-3-one (**1**) inhibited anti-CD28-induced IL-2 production and Abl tyrosine kinase with IC<sub>50</sub> values of 400 and 60 nM respectively. The 6*b*-stereoisomeric **2** was a moderate inhibitor of both IL-2 production and Abl tyrosine kinase while the 8-*oxo* derivative **3** was inactive in both assays. The 8-*O*-methyl ether **4** was a moderate inhibitor of IL-2 production but exhibited potent inhibition of Abl tyrosine kinase with an IC<sub>50</sub> of 45 nM.

The elucidation of intracellular signalling pathways triggered on initiation of an immune response provides new approaches to the identification of novel immunosuppressive agents for potential clinical development. T cells require two signals for activation: the first signal, to the T cell receptor (TCR), provided by the antigenic peptide/major histocompatibility complex (MHC) on antigen-presenting cells (APCs); and a co-stimulatory signal, mediated by the CD28 molecule on T cells on interaction with the B7-1 and B7-2 molecules on APCs.<sup>1)</sup> The key feature of the co-stimulatory signal mediated by CD28 is that, in conjunction with the TCR stimulus, it leads to high level interleukin-2 (IL-2) production. IL-2 is required for T cell survival and failure to produce adequate amounts of this cytokine, such as may occur in T cells responding to the first signal alone, leads to anergy.

Abrogation of co-stimulatory CD28 signalling thus represents a novel strategy for impeding T cell activation and to the induction of immunosuppression. With this objective in mind, a high throughput assay was developed to screen for inhibitors of anti-CD28-induced interleukin-2 (IL-2) production by Jurkat E6-1 cells as potential immunosuppressants.<sup>2)</sup> A series of compounds, the structures of which are shown in Fig. 1, with potent inhibitory effects on IL-2 production in this assay were isolated from fermentations of a microfungus whose taxonomic affinities are summarised as *Cladosporium* cf. *cladosporioides*. Further biological evaluation of the major active component, **1**, which has been reported elsewhere,<sup>2)</sup> established that **1** is a potent inhibitor of a range of tyrosine kinases but does not inhibit the serine-threonine kinase, protein kinase A. This article describes the taxonomic

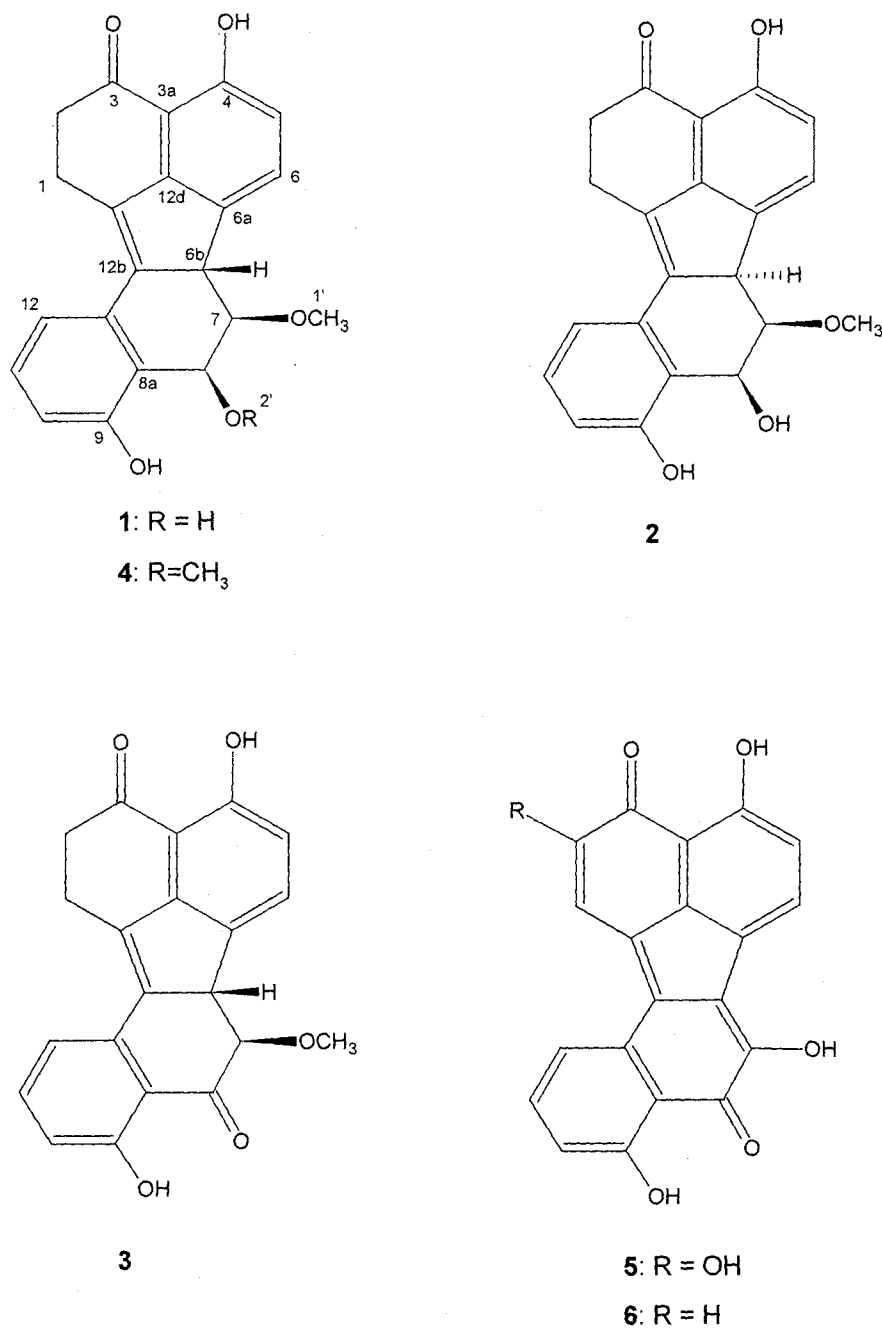
<sup>†</sup> Present address: Peptide Therapeutics, 321 Cambridge Science Park, Milton Road, Cambridge, CB4 4WG, UK.

<sup>††</sup> Present address: Astra Charnwood, Summerpool Road, Loughborough, Leics, LE11 5RH, UK.

<sup>†††</sup> Present address: Pfizer Ltd., Ramsgate Road, Sandwich, Kent, CT13 9NJ, UK.

\* Corresponding author: swrigley@cubist.com

Fig. 1. Structures of *Cladosporium* cf. *cladosporioides* metabolites 1~4 and *Bulgaria inquinans* metabolites bulgarhodin, 5, and bulgarein, 6.



characterisation and fermentation of *Cladosporium* cf. *cladosporioides* and the isolation, structure elucidation and effects on anti-CD28-induced IL-2 production and Abl tyrosine kinase of the novel reduced benzo[*j*]fluoranthren-3-ones 1~4.

## Experimental

### Source of Organism

The microfungus designated Cubist (formerly TerraGen and Xenova) Culture Collection number CBUK20700 was isolated directly from a dead insect colonised by a member

of the entomogenous fungus, genus *Hypocrella*. The insect was collected from tropical rain forest, Thailand, during 1989. The strain CBUK20700 was deposited under the Budapest Treaty at the Centraalbureau voor Schimmelcultures, Baarn, The Netherlands, on 25 November 1997, and was assigned the reference number CBS 100220.

#### Fermentation

The starting material for fermentation of this fungal strain was generated by suspending a mature slant culture, grown on a nutrient agar slope (2% malt extract, 0.1% peptone, 2% glucose, 1.5% agar), in 5 ml of 10% aqueous glycerol. This was stored at  $-135^{\circ}\text{C}$ . A preculture was produced by retrieving and thawing a 1 ml aliquot of starting material, aseptically placing it in 10 ml nutrient solution S1 (2% malt extract, 0.1% peptone, 2% glucose, adjusted to pH 6.0) and incubating for 10 days at  $25^{\circ}\text{C}$ . An intermediate culture was generated by transferring the preculture into a 250 ml flask containing 40 ml of nutrient solution S2 (1.5% glycerol, 1.5% soya bean peptone, 1% D-glucose, 0.5% malt extract, 0.3% NaCl, 0.1%  $\text{CaCO}_3$ , 0.1% Tween 80, 0.1% Junlon PW110 (supplied by Honeywell and Stein Ltd, Sutton, Surrey, UK), adjusted to pH 6.0) shaken at 240 rpm for three days at  $25^{\circ}\text{C}$ . A seed culture was generated by transferring the intermediate culture into 2 litres of nutrient solution S2 in a 3 litre fermenter. The fermenter was agitated at 500 rpm, aerated at 1 litre per minute and maintained at  $25^{\circ}\text{C}$  for three days. A production culture was generated by transferring the seed culture to a 75 litre fermenter containing 50 litres of nutrient solution P (2.6% trehalose, 0.5% yeast extract, 0.975% MES buffer, 0.1% Tween 80, 0.1% carboxymethyl cellulose, 0.1% antifoam A, adjusted to pH 6.0). The production fermenter was stirred at 350 rpm, aerated at 25 litres per minute, and the temperature controlled at  $25^{\circ}\text{C}$  for nine days, at which point the production culture was harvested and separated into liquor and biomass by passing it through a Westfalia disc-stack centrifuge.

#### Purification of Compounds 1~4

The fermentation supernatant was discarded and the biomass was extracted with 20 litres of a methanol/acetone (1 : 1) solvent mixture with continuous stirring in a mixing vessel for 3 hours after which the solvent extract was harvested *via* filtration. The retained biomass was transferred back to the mixing vessel and extracted again for a further 3 hours with 20 litres of methanol. The contents of the mixing vessel were then filtered. The combined solvent extracts (approximately 40 litres) were then evaporated to an aqueous concentrate (5 litres) using a

LUWA thin film evaporator and this was then extracted with 4×5 litres of ethyl acetate. The ethyl acetate extracts were pooled and evaporated to low volume (200 ml) under reduced pressure. This extract was then dried onto 40 g of loose silica (Sorbsil C60 40/60 Å) under reduced pressure and then fractionated by normal phase chromatography using a Biotage Flash 75L system with a SIM 500 module for sample introduction, a KP-Sil silica (32~62 µm 60Å) pre-packed column (i.d. 75×300 mm) using a stepwise gradient. The column was initially eluted with 100% hexane increasing to 100% ethyl acetate in 10% increments, with each step consisting of 1 litre elution volumes. The resultant fractions were analysed by reversed phased HPLC, using a Waters 600E HPLC system and 717 autosampler with a Waters C18 NovaPak (4 µm, 8×100 mm) radially compressed column and a water:acetonitrile gradient starting with a 2 minute hold at 90% water then increasing linearly to 100% acetonitrile over 13 minutes at 2 ml/minute. Fractions rich in target compounds were evaporated under reduced pressure to dryness and redissolved in 20~60 ml of methanol. HPLC analysis indicated that **1** eluted with 80 to 90% ethyl acetate from the flash column, **4** with 60% ethyl acetate, **2** with 50% ethyl acetate and **3** with 40% ethyl acetate.

Compound **1** was further purified by preparative reversed phase chromatography using a Biotage KP100 HPLC system with a Shandon hyperprep HS Bos 100Å 12 µm C18 column (i.d. 75×300 mm) and an isocratic mobile phase (60% water : 40% acetonitrile) with a flow rate of 350 ml/minute and dual wavelength UV detection at 300 and 400 nm. The peak collected after 9 minutes was evaporated to an aqueous phase and dried *in vacuo*, yielding 1.4 g of **1**.

Compounds **2** and **3** were purified by preparative reversed phase chromatography using a Waters Delta Prep HPLC system with a radially compressed 40×200 mm Prep NovaPak 60Å 6 µm C18 column and isocratic mobile phases comprising 52% water : 48% acetonitrile for **2** and 30% water : 70% acetonitrile for **3**. The flow rate was 55 ml/minute and UV detection was 340 nm. Compound **2** eluted after 8 to 8.5 minutes and **3** eluted after 6 to 6.5 minutes, both compounds were evaporated to an aqueous phase and then dried *in vacuo* to yield 20 mg of **2** and 40 mg of **3**.

Compound **4** was purified by semi-preparative reversed phase chromatography using a Waters 600E HPLC system with a radially compressed 25×200 mm Prep NovaPak 60Å 6 µm C18 column and an isocratic mobile phase comprising 55% water : 45% acetonitrile with a flow rate of 20 ml/minute and UV detection at 300 nm. The peak collected at 13.5 minutes was evaporated to an aqueous

phase and then dried *in vacuo* to yield 12 mg of 4.

#### Determination of Physico-chemical Properties

UV/visible spectra were measured on a Perkin-Elmer Lambda 17UV/visible spectrophotometer. IR spectra were recorded in KBr on a Nicolet 5PC FTIR spectrometer. Optical rotations were measured on a Bellingham and Stanley ADP220 polarimeter. Mass spectra were obtained on a Finnigan Mat 95 mass spectrometer.  $^1\text{H}$  and  $^{13}\text{C}$  NMR spectra were recorded at 308K on a Bruker ACF400 spectrometer at 400MHz and 100MHz respectively. All chemical shifts ( $\delta$ ) are quoted in ppm and are referenced to external TMS (Oppm). Standard techniques were used to obtain DEPT, COSY-45, HMQC, HMBC and NOESY NMR spectra. In the HMQC experiment the  $^1J_{\text{CH}}$  was optimised for 145 Hz. In HMBC experiments the long range coupling constant  $^3\text{--}5J_{\text{CH}}$  was optimised for 7 Hz and 3 Hz. A mixing time of 1.4 seconds was used in the NOESY experiment.

#### Cells and Culture Conditions

Jurkat E6-1 cells obtained from the European Collection of Cell Cultures (ECACC) were maintained in RPMI 1640 medium (RPMI) with 5% fetal bovine serum (FBS). These cells were primarily used in the screening assay for the identification of inhibitors of PMA and anti-CD28 induced IL-2 production. Jurkat E6-1 cells were resuspended at  $1 \times 10^6$ /ml in fresh RPMI with 5% FBS and exposed to 3 ng/ml PMA for 3 hours at 37°C with 5%  $\text{CO}_2$ . Cells were washed, resuspended at  $1 \times 10^6$ /ml in fresh RPMI with 5% FBS, aliquoted at 200  $\mu\text{l}$ /well into 96 well Plates (Gibco, UK) and test compounds added at optimal concentrations. Following an overnight incubation at 37°C with 5%  $\text{CO}_2$ , anti-CD28 antibody (Ancell, UK) at a final concentration of 2  $\mu\text{g}/\text{ml}$  was added and incubated for another 20 hours at 37°C with 5%  $\text{CO}_2$ . The IL-2 concentration in the cell culture supernatants was determined by DELFIA as described below.

#### Cytokine Dissociation Enhanced Lanthanide Fluorescence Immunoassay (DELFIA)

Ninety-six well plates (Greiner, UK) were coated with 5  $\mu\text{g}/\text{ml}$  anti-human IL-2 monoclonal antibody (R&D Systems) in PBS at 4°C overnight. Blocking buffer (1% BSA in PBS) was added for one hour followed by the addition of samples or recombinant IL-2 standard (R&D Systems) and incubation for 2 hours. Polyclonal sheep anti-human IL-2 (NIBSC, UK) diluted in Assay buffer (Wallac, Finland) with 5% normal human serum was added for one hour. Then rabbit anti-sheep biotin conjugated IgG (Vector,

USA) in Assay buffer was added for one hour followed by the addition of streptavidin conjugated europium (Wallac) for 30 minutes. The fluorescence counts due to europium were determined after the addition of Enhancement Solution (Wallac) using the Victor 1420 (Wallac). Jurkat E6-1 cells in the presence of medium alone did not produce detectable levels of IL-2 and after stimulation the IL-2 concentrations detected were in the range  $20 \pm 0.4$  ng/ml.

#### Kinase Assays

The effect on Abl kinase activity was evaluated using a homogeneous time resolved fluorescence assay (HTRF). 0.5  $\mu\text{g}/\text{ml}$  biotin labeled p34 cdc2(6-20aa) peptide (Pierce, UK) was incubated in the presence of purified compounds at concentrations between 0.01~5  $\mu\text{M}$ , 10 units of Abl tyrosine kinase (Calbiochem, UK) in 50  $\mu\text{l}$  of enzyme kinase buffer (50 mM HEPES pH 7.4, 10 mM  $\text{MgCl}_2$ , 2 mM DTT, 0.03% BSA, 0.01% BRIJ, 20  $\mu\text{M}$  ATP) for 3 hours at 30°C. The reaction was stopped by the addition of 2.5 mM EDTA and phosphorylation on tyrosine residues detected following the addition of europium labeled anti-phosphotyrosine (PT66-Eu, Wallac) and streptavidin labeled allophycocyanin (Strep-APC, Wallac) in TBS-BSA (50 mM Tris-HCl, pH 7.4, 150 mM NaCl, 0.5% BSA, 0.1% sodium azide) and incubation for 10 minutes at 30°C. Fluorescence counts due to Eu-APC energy transfer were determined using the Victor 1420 (Wallac).

## Results

### Taxonomy of Fungus CBUK20700

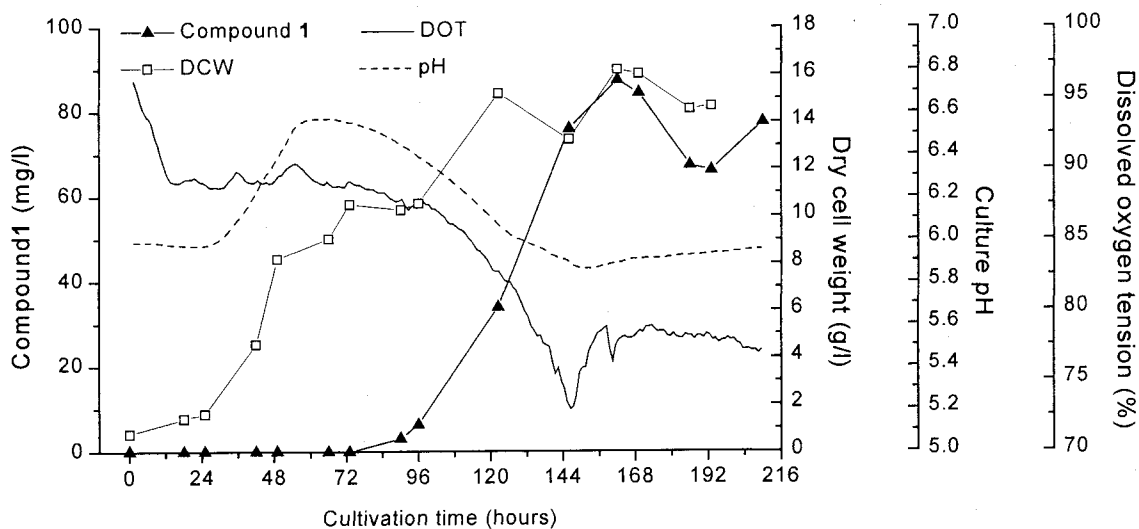
This fungus was readily assignable to the widespread hyphomycete genus *Cladosporium* Link ex Fr. on the basis of the morphological data shown in Table 1 following inoculation of its conidia at the centre of Petri dishes containing 2% malt extract (Difco Laboratories) agar. No growth was observed at 37°C. Although this genus is associated with the ascomycete family Mycosphaerellaceae (order Dothideales), no sexually reproducing state was observed in culture. Generally, all cultures had submerged mycelial margins and radially sulcate central regions supporting very sparse sporulation. Microscopically, the conidiophores were usually septate with thick brown walls at their base tapering and becoming progressively thinner-walled and paler towards their apices. The apices were usually slightly swollen at the point of attachment of the lowermost conidia (ramo-conidia). Ramo-conidia were very rarely 1-septate and formed the main branches of a loose head of branched acropetally extending chains of aseptate

Table 1. Macroscopic and microscopic characteristics of fungus CBUK20700 on 2% malt extract agar following incubation at 24°C.

7-Day mycelial diameter (mm)	6~7
Mycelial texture	Abundant dense aerial mounds
Main colony colours* (above)	Olivaceous buff, grey olivaceous
Main colony colours* (below)	Olivaceous black, fuscous black
Main colours* of aerial droplets	9H (ochreous)
Conidiophore length ( $\mu$ )	19 ~ 240
Max. conidiophore width ( $\mu$ )	<5
Conidial form	Mostly smooth, fusiform or limoniform
Ramo-conidial length ( $\mu$ )	<16
Ramo-conidial width ( $\mu$ )	2.5 ~ 4.0
Conidial length ( $\mu$ )	3 ~ 6.5
Conidial width ( $\mu$ )	1.5 ~ 3.5

\* Colours according to ANON.<sup>3)</sup>

Fig. 2. Typical fermentation timecourse for the production of compound 1 by *Cladosporium cf. cladosporioides*.



conidia with apiculate ends.

Although the cultures exhibited many morphological characters of *Cladosporium cladosporioides* (Fres.) de Vries, nevertheless their reduced mycelial extension rate and much sparser conidiogenesis were outside the usual range for this taxon. Furthermore, four other fungal isolates originating from similar Thai source materials (two collected during the following year in 1990) had similar taxonomic characters and also produced compound 1 when fermented. By contrast, 1 was not detected following fermentation of an authentic strain of *C. cladosporioides*.

Hence the taxonomic status of CBUK20700 was expressed as *Cladosporium cf. cladosporioides*, possibly an ecologically specialized variant naturally associated with other entomogenous fungi.

#### Fermentation

The changes in dry cell weight, pH, dissolved oxygen tension and titre of 1 that occurred during a typical fermentation of *Cladosporium cf. cladosporioides* CBUK20700 are shown in Fig. 2.

Table 2. Physicochemical properties of *Cladosporium* cf. *cladosporioides* metabolites 1~4.

	1	2	3	4
Appearance	Yellow powder	Yellow powder	Yellow powder	Yellow powder
DCI-MS (m/z)	351 (MH <sup>+</sup> ) 333 ([MH-H <sub>2</sub> O] <sup>+</sup> )	351 (MH <sup>+</sup> ) 333 ([MH-H <sub>2</sub> O] <sup>+</sup> )		
DEI-MS (m/z)	350 (M <sup>+</sup> ) 352 ([M-H <sub>2</sub> O] <sup>+</sup> )	350 (M <sup>+</sup> ) 352 ([M-H <sub>2</sub> O] <sup>+</sup> )	348 (M <sup>+</sup> )	364 (M <sup>+</sup> )
Molecular formula	C <sub>21</sub> H <sub>18</sub> O <sub>5</sub>	C <sub>21</sub> H <sub>18</sub> O <sub>5</sub>	C <sub>21</sub> H <sub>16</sub> O <sub>5</sub>	C <sub>22</sub> H <sub>20</sub> O <sub>5</sub>
HREI-MS Found:	350.1150	350.1143	348.0985	364.1317
Calculated:	350.1154	350.1154	348.0998	364.1311
UV-vis λ <sub>max</sub> /nm (MeOH)	212, 255, 307, 382	212, 255, 307, 382	240, 271, 290, 304, 401	212, 355, 307, 382
[α] <sub>D</sub> <sup>20</sup>	-81° (c 0.25, CH <sub>2</sub> Cl <sub>2</sub> )	-	-270° (c 0.03, CH <sub>2</sub> Cl <sub>2</sub> )	-
IR (KBr) ν /cm <sup>-1</sup>	3423, 2927, 2854, 1706, 1641, 1605, 1579, 1470, 1345, 1277, 1229, 1194, 1118, 1094	3273, 2913, 2844, 1701, 1645, 1604, 1569, 1445, 1410, 1348, 1325, 1275, 1209, 1190, 1161, 1130, 1125, 1071, 1008	2962, 2927, 2858, 2830, 1708, 1645, 1604, 1555, 1458, 1348, 1334, 1275, 1195, 1161	3245, 3052, 2934, 2823, 1632, 1569, 1458, 1327, 1271, 1223, 1188, 1091, 1043, 731

### Structure Elucidation

The physico-chemical properties, <sup>1</sup>H and <sup>13</sup>C NMR spectral data for compounds 1~4 are summarized in Tables 2~4 respectively. Compound 1 was the main active component detected in fermentations of *Cladosporium* cf. *cladosporioides*. The electron impact mass spectrum gave a molecular ion at *m/z* 350. A high resolution mass measurement of this ion was consistent with the molecular formula C<sub>21</sub>H<sub>18</sub>O<sub>5</sub>. The <sup>1</sup>H and <sup>13</sup>C NMR data for 1 are summarized in Tables 3 and 4. The <sup>13</sup>C NMR spectrum confirmed the presence of 21 carbon atoms and DEPT spectra indicated that these comprised 1 methyl, 2 methylene, 8 methine and 10 quaternary carbons. An HMQC (<sup>1</sup>H-<sup>13</sup>C correlation spectrum) experiment established the one bond connectivities of the proton and carbon atoms. Inspection of the chemical shift data indicated that the 63.9 and 82.0 ppm methine carbons and the quaternary carbons at 156.6, 159.2 and 201.7 ppm were attached to oxygen. Further inspection of <sup>1</sup>H-<sup>1</sup>H coupling constants, 2D-COSY data and long range H-C couplings

detected in heteronuclear multiple bond connectivity (HMBC) experiments, together with consideration of <sup>1</sup>H and <sup>13</sup>C chemical shift data indicated several structural moieties. The two methylene groups at 3.35/22.8 and 2.88/36.5 ppm were obviously adjacent and in close proximity to the carbonyl carbon at 201.7 ppm, as were two *ortho*-coupled aromatic methines at 6.76/113.5 and 7.70/133.0 ppm. A second aromatic system was indicated by three more adjacent aromatic methines at 6.91/116.2, 7.30/130.1 and 7.21/118.5 ppm. The <sup>1</sup>H-<sup>1</sup>H coupling constants for the methines at 3.99/49.6, 3.22/82.0 and 5.39/63.9 ppm indicated that these were contiguous and the methoxyl group at 3.55/58.1 ppm was linked in to this system by an HMBC correlation to 82.0 ppm. At this stage searching of the Chapman and Hall Dictionary of Natural Products<sup>4)</sup> for fungal metabolites with similar molecular formulae and the general structural features described above suggested that 1 was closely related to two benzofluoranthenequinone metabolites, bulgarhodin and bulgarein, of the fungus *Bulgaria inquinans*.<sup>5)</sup> These two compounds have highly unsaturated pentacyclic structures.

Table 3.  $^1\text{H}$  NMR assignments of 1~4 in  $\text{CDCl}_3$  solutions (400 MHz).

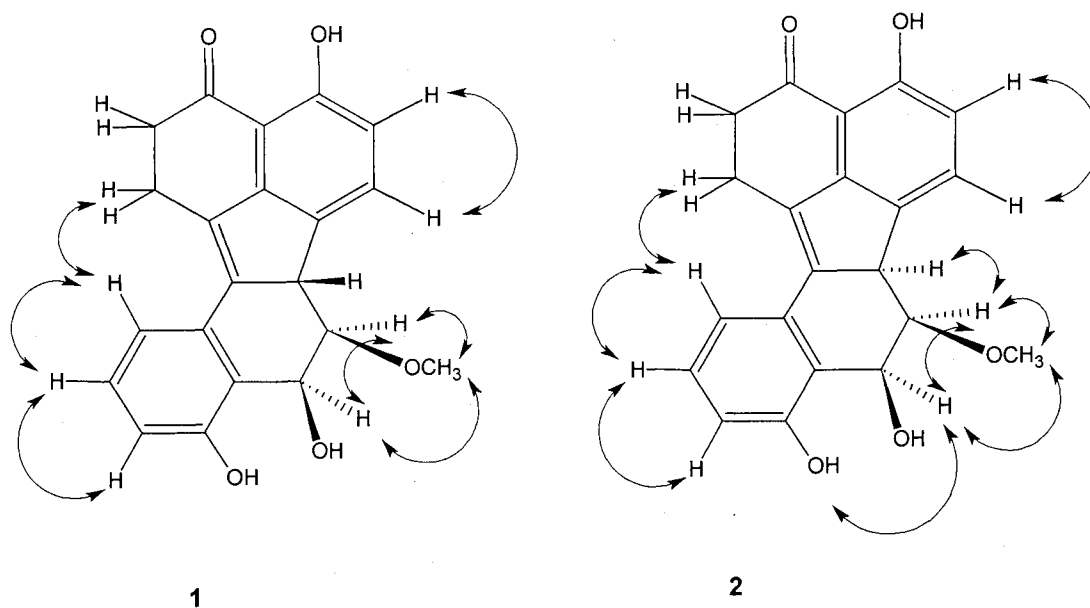
Position	1	2	3	4
1	3.35 (2H, m)	3.40 (2H, m)	3.35 (2H, m)	3.25 (1H, m), 3.35 (1H, m)
2	2.88 (2H, m)	2.90 (2H, m)	2.95 (2H, m)	2.85 (2H, m)
3				
3a				
4	10.6 (1H, s, OH)	10.69 (1H, s, OH)	10.6 (1H, s, OH)	10.6 (1H, s, OH)
5	6.76 (1H, d, 8.1)	6.76 (1H, d, 8.2)	6.85 (1H, d, 8.3)	6.75 (1H, d, 8.2)
6	7.70 (1H, d, 8.2)	7.63 (1H, d, 8.2)	7.70 (1H, d, 8.2)	7.80 (1H, d, 8.2)
6a				
6b	3.99 (1H, dt, 11.9, 2.4)	3.78 (1H, bd, 2.2)	4.15 (1H, dt, 12.7, 2.4)	4.30 (1H, dt, 11.8, 2.5)
7	3.22 (1H, dd, 11.9, 4.2)	4.51 (1H, dd, 4.2, 2.0)	3.55 (1H, d, 12.7)	3.15 (1H, dd, 11.8, 3.5)
8	5.39 (1H, d, 4.1)	5.23 (1H, dd, 10.7, 3.8) 3.52 (1H, bd, 11.3, OH)		5.20 (1H, d, 3.5)
8a				
9		8.77 (1H, s, OH)	12.2 (1H, s, OH)	
10	6.91 (1H, d, 8.0)	6.90 (1H, dd, 8.0, 1.0)	6.90 (1H, d, 8.3)	6.80 (1H, dd, 6.9, 2.0)
11	7.30 (1H, d, 7.9)	7.27 (1H, t, 7.9)	7.50 (1H, t, 8.0)	7.25 (2H, m)
12	7.21 (1H, d, 7.8)	7.20 (1H, dd, 7.0, 1.0)	7.10 (1H, d, 7.4)	7.25 (2H, m)
12a				
12b				
12c				
12d				
1'	3.55 (3H, s)	3.08 (3H, s)	3.75 (3H, s)	3.55 (3H, s) 3.70 (3H, s)

\* Coupling constants given in Hz in parentheses

Table 4.  $^{13}\text{C}$  NMR assignments of 1~4 in  $\text{CDCl}_3$  solutions (100 MHz).

Position	1	2	3	4
1	22.8	23.1	22.9	23.1
2	36.5	36.6	36.3	36.5
3	201.7	201.9	201.3	201.8
3a	112.4	112.7	112.7	112.2
4	159.2	159.5	159.6	159.1
5	113.5	112.9	114.5	113.4
6	133.0	130.3	132.9	133.5
6a	132.9	132.1	134.0*	133.6
6b	49.6	53.9	55.2	50.7
7	82.0	81.1	85.0	83.8
8	63.9	70.8	204.1	71.4
8a	123.0	120.6	114.3	122.7
9	156.6	158.3	163.4	155.5
10	116.2	117.2	117.6	115.1
11	130.1	129.5	137.1	129.8
12	118.5	118.0	117.0	118.9
12a	133.1	131.7	137.5	134.4
12b	139.9	138.2	136.0	140.5
12c	131.3	131.0	133.8*	131.3
12d	150.9	151.7	150.1	150.5
1'	58.1	61.8	60.6	57.8
2'	-	-	-	58.9

\* Assignments interchangeable

Fig. 3. NOE's observed in the NOESY NMR spectra of **1** and **2**.

The long range  $^1\text{H}$ - $^{13}\text{C}$  correlations observed in the HMBC NMR spectra of **1** were found to be consistent with a structure based on the same carbon skeleton as found in bulgarhodin, **5**, and bulgarein, **6**. These structures are shown in Figure 1. The stereochemistry for **1** indicated in Figure 1 is relative and was determined by inspection of  $^1\text{H}$ - $^1\text{H}$  coupling constants and nuclear Overhauser effects observed in a NOESY NMR experiment (Fig. 3). This structure was subsequently confirmed by X-ray crystallography (data not shown). Compound **1** is thus (6*b**S*,7*R*,8*S*)-7-methoxy-4,8,9-trihydroxy-1,6*b*,7,8-tetrahydro-2*H*-benzo[*j*]fluoranthren-3-one.

The molecular formula and UV-visible spectrum of compound **2** were identical with those of **1**. The main differences in the  $^1\text{H}$  and  $^{13}\text{C}$  NMR spectra of **2** compared to **1** were found in the coupled system of methines at positions 6*b*, 7 and 8. The hydroxyl proton at position 8 gave a distinct  $^1\text{H}$  NMR signal at 3.52 ppm (not observed in the  $^1\text{H}$  NMR spectrum of **1**) with a  $^1\text{H}$ - $^1\text{H}$  coupling constant to 8-H of 11 Hz. The  $^1\text{H}$ - $^1\text{H}$  coupling constant between the protons at positions 7 and 8 in **2** (4.0 Hz) was similar to that of **1** (4.1 Hz). The  $^1\text{H}$ - $^1\text{H}$  coupling constant between the protons at positions 6*b* and 7, however, was much smaller in **2** (2.0 Hz) than in **1** (11.9 Hz), indicating a *cis*- as opposed to *trans*- stereochemical relationship. Further support for this assignment was obtained through a NOESY NMR experiment (Fig. 3). Compound **2** is thus

(6*b**R*,7*R*,8*S*)-7-methoxy-4,8,9-trihydroxy-1,6*b*,7,8-tetrahydro-2*H*-benzo[*j*]fluoranthren-3-one.

Compound **3** had a molecular weight of 348 and HREI-MS indicated a molecular formula of  $\text{C}_{21}\text{H}_{16}\text{O}_5$ . Its UV-visible spectrum indicated a more highly conjugated chromophore. Inspection of the  $^1\text{H}$  and  $^{13}\text{C}$  NMR spectra of **3** indicated that position 8 was now oxidized to a carbonyl compared with **1** and **2**, the carbon shift at this position being 204.1 ppm. The 9-hydroxyl proton was now evident as a sharp, hydrogen-bonded singlet at 12.2 ppm. The  $^1\text{H}$ - $^1\text{H}$  coupling constant between the protons at positions 6*b* and 7 (12.7 Hz) was similar to that observed in **1** (11.9 Hz), indicating the same *trans*-stereochemical arrangement. Compound **3** is thus (6*b**S*,7*R*)-4,9-dihydroxy-7-methoxy-1,2,6*b*,7-tetrahydrobenzo[*j*]fluoranthren-3,8-dione.

Compound **4** had a molecular weight of 364 and HREI-MS indicated a molecular formula of  $\text{C}_{22}\text{H}_{20}\text{O}_5$ . Its UV-visible spectrum was identical to that of **1**. The  $^1\text{H}$  and  $^{13}\text{C}$  NMR spectra of **3** were almost identical with those of **1** except for signals at 3.70 and 58.9 ppm indicating an extra methoxyl moiety. Correlations between the new methoxyl proton signal and the carbon at 71.4 ppm and between the 8-methine proton signal at 5.20 ppm and the new methoxyl carbon at 58.9 ppm observed in an HMBC NMR experiment optimized for 3 Hz indicated that the 8-hydroxyl of **1** was now methylated (there was a corresponding correlation from the methoxyl proton signal



at 3.55 ppm to the carbon at 83.8 ppm). The  $^1\text{H}$ - $^1\text{H}$  coupling constants between the protons at positions 6b, 7 and 8 were very similar to those for **1**, indicating the same stereochemical arrangement. Compound **4** was therefore (6*S*,7*R*,8*S*)-4,9-dihydroxy-7,8-dimethoxy-1,6b,7,8-tetrahydro-2*H*-benzo[*j*]fluoranthren-3-one.

### Biological Activity

The  $\text{IC}_{50}$  values of compounds **1**~**4** for the inhibition of anti-CD28-induced IL-2 production by Jurkat E6-1 cells and for inhibition of Abl tyrosine kinase are shown in Table 4. Compound **1** is the most active of the four, inhibiting IL-2 production and tyrosine kinase activity with  $\text{IC}_{50}$ 's of 400 and 60 nM respectively. Its stereoisomer, **2**, is six-fold less active in the IL-2 production assay and over ten-fold less active as an Abl tyrosine kinase inhibitor. Oxidation at position 8 (compound **3**) results in no detectable activity in either assay at a concentration of 5  $\mu\text{M}$ . Methylation of the hydroxyl group at position 8 (compound **4**) results in a slightly more potent  $\text{IC}_{50}$  for inhibition of Abl tyrosine kinase than **1** but a six-fold less potent effect on inhibition of anti-CD28-induced IL-2 production. This could be accounted for by changes in compound solubility and intracellular distribution. The detailed biological evaluation of **1** has been reported elsewhere.<sup>2)</sup>

### Discussion

A high throughput screening assay based on IL-2 production by Jurkat E6-1 cells was used to screen approaching 100,000 microbial fermentation extracts for inhibitors of CD28 signal transduction. Extracts of one particular strain (Cubist (formerly TerraGen and Xenova) culture collection number CBUK20700) were found to cause potent inhibition of anti-CD28 stimulated IL-2 production with no toxic effects observed on Jurkat E6-1 cells. This strain has been taxonomically classified as *Cladosporium* cf. *cladosporioides*. Members of the compound series responsible for this activity have been identified as the novel reduced benzo[*j*]fluoranthren-3-ones **1**~**4**. These are related to two other pentacyclic, benzofluoranthenequinone metabolites, bulgarein and bulgarhodin, of the fungus *Bulgaria inquinans*,<sup>5)</sup> but are distinguished structurally from these two compounds by several reduction steps and one *O*-methylation step. Compound **1** was the most potent inhibitor of anti-CD28-induced IL-2 production and, in addition to inhibiting Abl tyrosine kinase, was also found to inhibit other tyrosine

Table 5.  $\text{IC}_{50}$  values of compounds **1**~**4** for the inhibition of anti-CD28-induced IL-2 production by Jurkat E6-1 cells and for inhibition of Abl tyrosine kinase.

Compound	$\text{IC}_{50}$ ( $\mu\text{M}$ )	
	Anti-CD28 -induced IL-2 production in Jurkat E6-1 cells	Abl tyrosine kinase
<b>1</b>	0.4	0.06
<b>2</b>	2.5	0.76
<b>3</b>	>5.0	>5.0
<b>4</b>	2.4	0.045

kinases, including Fyn, Lck and epidermal growth factor receptor (EGFR) tyrosine kinases, with  $\text{IC}_{50}$  values in the range 20~400 nM.<sup>2)</sup> Compound **1** was not found to have any effects in an assay for inhibition of the serine-threonine kinase, protein kinase A and there is indirect evidence that **1** does not inhibit protein kinase C.<sup>2)</sup> Other selective tyrosine kinase inhibitors of microbial origin include the *Streptomyces* sp. metabolite erbstatin, which was isolated as an inhibitor of epidermal growth factor receptor (EGFR) tyrosine kinase;<sup>6,7)</sup> lavendustin A, another, potent, EGFR tyrosine kinase inhibitor from *Streptomyces griseolavendus*;<sup>8)</sup> BE-23372M, an EGFR tyrosine kinase inhibitor from *Rhizoctonia solani*;<sup>9)</sup> hibarimicins, Src tyrosine kinase inhibitors from *Microbispora rosea* subsp. *hibaria*;<sup>10)</sup> and L-783,277 and related resorcylic acid lactones isolated as MEK (MAPK/ERK kinase, Mitogen activated protein kinase/Extracellular signal-related kinase Kinase) inhibitors from a *Phoma* sp.<sup>11)</sup> Compounds **1**~**4** differ structurally from these and thus represent a new chemical class of tyrosine kinase inhibitors. It is noteworthy that the calphostins from *Cladosporium cladosporioides* were reported as specific inhibitors of protein kinase C versus protein kinase A,<sup>12,13)</sup> without any inhibitory effects on a tyrosine-specific kinase.<sup>14)</sup> In addition to being produced by a closely-related fungus, the calphostins have some superficial structural similarities to compounds **1**~**4** as they are based on an oxygenated pentacyclic core structure. Both series of compounds are protein kinase inhibitors and yet have very different selectivity properties.

## Acknowledgements

We are grateful to Drs. MASASHI MATSUI, TOSHIO TATSUOKA and YASUNORI TAWARAGI of SUNTORY LTD., Institute of Biomedical Research for discussions during the course of this work. We would like to acknowledge TREVOR GIBSON for providing mass spectra and MOHAMMED LATIF for NMR spectra.

## References

- 1) WARD, S. G.: CD28: a signalling perspective. *Biochem. J.* 318: 361~377, 1996
- 2) SADHEGHI, R.; P. DEPLEGGE, P. RAWLINS, N. DHANJAL, A. MANIC, S. WRIGLEY, B. FOXWELL & M. MOORE: Differential regulation of CD3- and CD28-induced IL-2 and IFN $\gamma$  production by a novel tyrosine kinase inhibitor XR774 from *Cladosporium* cf. *cladosporioides*. *Int. Immunopharmacol.* 1: 33~48, 2001
- 3) ANON: Flora of British Fungi: Colour identification chart. H.M.S.O., Edinburgh U.K. 1969
- 4) Dictionary of Natural Products on CD-ROM, Chapman & Hall/CRC Press, Boca Raton, London, Washington DC
- 5) EDWARDS, R. L. & H. J. LOCKETT: Constituents of the higher fungi Part XVI Bulgarhodin and bulgarein, novel benzofluoranthenequinones from the fungus *Bulgaria inquinans* (Fries). *J. Chem. Soc. Perkin Trans 1*: 2149~2155, 1976
- 6) UMEZAWA, H.; M. IMOTO, T. SAWA, K. ISSHIKI, N. MATSUDA, T. UCHIDA, H. IINUMA, M. HAMADA & T. TAKEUCHI: Studies on a new epidermal growth factor-receptor kinase inhibitor, erbstatin, produced by MH435-hF3. *J. Antibiotics* 39: 170~173, 1986
- 7) OIKAWA, T.; H. ASHINO, M. SHIWAMURA, M. HASEGAWA, I. MORITA, S.-I. MUROTA, M. ISHIZUKA & T. TAKEUCHI: Inhibition of angiogenesis by erbstatin, an inhibitor of tyrosine kinase. *J. Antibiotics* 46: 785~790, 1993
- 8) ONODA, T.; H. IINUMA, Y. SASAKI, M. HAMADA, K. ISSHIKI, H. NAGANAWA, T. TAKEUCHI, K. TATSUKA & K. UMEZAWA: Isolation of a novel tyrosine kinase inhibitor, lavendustin A, from *Streptomyces griseolavendus*. *J. Nat. Prod.* 52: 1252~1257, 1989
- 9) OKABE, T.; E. YOSHIDA, S. CHIEDA, K. ENDO, S. KAMIYA, K. OSADA, S. TANAKA, A. OKURA & H. SUDA: BE-23372M, a novel protein tyrosine kinase inhibitor. I. Producing organism, fermentation, isolation and biological activities. *J. Antibiotics* 47: 289~293, 1994
- 10) KAJIURA, T.; T. FURUMAI, Y. IGARASHI, H. HORI, K. HIGASHI, T. ISHIYAMA, M. URAMOTO, Y. UEHARA & T. OKI: Signal transduction inhibitors, hibarimicins A, B, C, D and G produced by *Microbispora* I. Taxonomy, fermentation, isolation and physico-chemical and biological properties. *J. Antibiotics* 51: 394~401, 1998
- 11) ZHAO, A.; S. H. LEE, M. MOJENA, R. G. JENKINS, D. R. PATRICK, H. E. HUBER, M. A. GOETZ, O. D. HENSENS, D. L. ZINK, D. VILELLA, A. W. DOMBROWSKI, R. B. LINGHAM & L. HUANG: Resorcylic acid lactones: naturally occurring potent and selective inhibitors of MEK. *J. Antibiotics* 52: 1086~1094, 1999
- 12) KOBAYASHI, E.; K. ANDO, H. NAKANO & T. TAMAOKI: UCN-1028A, a novel and specific inhibitor of protein kinase C, from *Cladosporium*. *J. Antibiotics* 42: 153~155, 1989
- 13) KOBAYASHI, E.; K. ANDO, H. NAKANO, T. IIDA, H. OHNO, M. MORIMOTO & T. TAMAOKI: Calphostins (UCN-1028), novel and specific inhibitors of protein kinase C I. Fermentation, isolation, physico-chemical properties and biological activities. *J. Antibiotics* 42: 1470~1474, 1989
- 14) KOBAYASHI, E.; H. NAKANO, M. MORIMOTO & T. TAMAOKI: Calphostin C (UCN-1028C), a novel microbial compound, is a highly potent and specific inhibitor of protein kinase C. *Biochem. Biophys. Res. Comm.* 159: 548~553, 1989